Results

Hypoxia elongated growth of MSCs

MSCs were isolated from bone marrow of four donors, designated hBM66, hBM72, hBM77, and hBM80, respectively, and cultured under normoxic or hypoxic conditions as described in Materials and Methods. In the case of hBM66, there was no significant difference between normoxic and hypoxic cultured-cells in terms of growth profile until PD15 (Fig. 1). After this stage, normoxic cultured-cells ceased to proliferate, whereas hypoxic cultured-cells kept on growing, and the number of PD at the last observation under normoxic and hypoxic conditions was 24 and 40, respectively. The theoretically accumulated cell number was 65,000-fold higher in the hypoxic culture. Similar results were obtained with the other three hBM cells (Fig. 1), and the final number of PD in normoxic- and hxpoxic-cultured cells was 17 and 25 in hBM72, 25 and 39 in hBM77, and 24 and 45 in hBM80.

Hypoxia rescued MSCs from cellular senescence

In the case of hBM77, most of the normoxic cultured-cells at PD25 were positive for SA-β-gal, whereas few were stained in the hypoxic culture at PD28 (Fig. 1B), and the difference was highly significant (Fig. 1C). Similar results were obtained with the other three hBM cells (Fig. 1C), indicating that the hypoxic culture protected MSCs from cellular senescence, which may be the cause of the increase in life span *in vitro*.

Hypoxia inhibited the up-regulation of p16 expression

We have demonstrated that the induction of cellular senescence in MSCs is tightly associated with the up-regulation of *p16* gene expression [20]. Consistent with previous findings, the level of p16 increased with the life span of normoxic cultured-hBM66, which was seven-times higher at PD20 than at PD3 (Fig. 2, upper panel). In contrast, hypoxic cultured-hBM66 retained a lower level of the p16 expression, which was only two-times higher at PD20 than at PD3 (Fig. 2, upper panel). Similar results were obtained with the other three hBM cells (Fig. 2), suggesting that hypoxia inhibited the induction of *p16* gene expression, which then protected cells from cellular senescence.

Hypoxia affected the ability to differentiate into chondro- and adipogenic, but not osteogenic, lineage.

The ability to differentiate into osteo-, chondro-, and adipogenic lineages in the early phase was confirmed in all four hBM cells (data not shown). After long-term culture (about 100 days), no significant difference in osteogenic differentiation, measured based on Ca content, was observed between normoxic and hypoxic cultured-MSCs (Fig. 3A). In contrast, the ability to differentiate into the chondrogenic (Fig. 3B) and adipogenic (Fig. 3C) lineages, measured from GAG and TG content respectively, was significantly more superior in hypoxic than normoxic conditions.

Hypoxia inhibited the activation of ERK

In the case of hBM66, the expression of molecules related to MAPK signals showed no significant difference between normoxic and hypoxic cultured-cells

except that of ERK (Fig. 4A). Levels of both phospho-ERK1 and phospho-ERK2 were much lower in hypoxic cultured-cells than in normoxic cultured-cells throughout the culture period, and similar results were obtained with the other three hBM cells (Fig. 4B). nPG is an antioxidant, which induces the production HIF-1α protein [24]. Treatment of hBM72 cells (PD3) cultured under normoxic conditions with nPG successfully induced the expression of HIF-1α, but failed to reduce the level of phospho-ERK1/2 (Fig. 4C), indicating that the reduction in phospho-ERK is not a direct consequence of HIF-1α's activation. To investigate the relationship between ERK and p16, the activity of MEK, by which ERK is phosphorylated, was inhibited by U0126. When hBM72 cells (PD3) cultured under normoxic conditions were treated with U0126 for four days, activation of ERK was inhibited throughout the culture period (Fig. 4D). During this period, the level of *p16* increased two-fold in control cells, but only slightly in U0126 treated-cells (Fig. 4D), suggesting that the ERK signal is one of the factors inducing the expression of the *p16* gene.

Discussion

A number of studies have been published regarding the effects of hypoxia on the growth and differentiation of MSCs [12-17], but the results differed considerably. The discrepancies may be at least in part due to differences in species, the concentration of oxygen, and/or the length of culture periods, and the discussion hereafter focuses on the data for human MSCs. As for short-term effects, some studies showed that hypoxia increased the proliferation of MSCs by promoting progression of the cell cycle [16], but others showed no or even the opposite effect [14], consistent with the results of the current study. Two studies have analyzed the long-term effects of hypoxia on human MSCs. Grayson *et al.* showed that human MSCs displayed enhanced proliferation under hypoxic conditions (2% pO_2) for seven passages over six weeks, resulting in a 30-fold increase in cell number compared with that under normoxic conditions [15]. Fehrer *et al.* showed that MSCs cultured under hypoxic conditions (3% pO_2) for up to 100 days had a higher number of final PD than those cultured under normoxic conditions by ten [17], which agreed with the results of the current study. Because the PD time showed no difference during the early phase of growth (Fig. 1A), our data indicate that hypoxia did not affect the growth of cells, but extended their life span, and the marked difference in the number of SA-β-gal-positive cells between hypoxic and normoxic conditions clearly indicates that the lengthening of life span by hypoxia is due to the escape from cellular senescence. We have shown that the up-regulation of p16 gene

expression is key to inducing cellular senescence in human MSCs [20]. In the current study, we showed that hypoxia inhibited the up-regulation of p16 gene expression. ROS induces p16 gene expression [21,22], and the p16-Rb pathway then induces the production of ROS, which leads to cellular senescence [25].

Regarding the effects of hypoxia on the differentiation of MSCs, published results vary. To evaluate the ability of MSCs to differentiate, osteo-, chondro-, or adipogenic differentiation has been analyzed in most studies [12-17], but no studies have examined all three lineages in MSCs cultured under hypoxic conditions long term. Martin-Rendon *et al.* analyzed the short-term effects (24 hours) of hypoxia (1% pO_2) on the differentiation into three lineages and found that only chondrogenic differentiation was improved [16]. Our data indicated that chondrogenic, as well as adipogenic, but not osteogenic, differentiation was improved in MSCs cultured under hypoxic conditions for long term (about 100 days). Although the molecular mechanisms underlying this change in the behavior of MSCs are not known, the down-regulation of phospho-ERK expression caused by a reduction in oxygen is an intriguing new finding of the current study. MAPK signaling pathways have profound effects on the growth and differentiation of MSCs [26,27], and the signaling through ERK has been investigated intensively. Activation of the ERK signal triggers osteogenic differentiation [28,29]. The up-regulation of MAPK signals promoted chondrogenesis by inducing the expression of the *Sox9* gene [30].

The inhibition of ERK signals reduced the adipogenic differentiation [31]. Therefore, the ERK signal is essential to the differentiation of MSCs. In other words, inhibition of the ERK signal may restrict the "spontaneous" differentiation which maintains MSC in an undifferentiated state. The ERK signal also plays a role as a mitogenic stimulus, which promotes growth, but at the same time induces cellular senescence of MSCs. Inhibition of the ERK signal by a MEK inhibitor reduced the up-regulation of p16 gene expression. Therefore, down-regulation of phospho-ERK expression may also help cells to escape from cellular senescence during propagation *in vitro*. Further study of mechanisms by which hypoxia down-regulates the ERK signal may provide a new method of culturing MSCs.

Acknowledgements

We are grateful to Drs. Y. Shima, K. R. Shibata, K. Fukiage, and K. Hirota for technical support, and M. Neo and S. Fujibayashi for recruiting donors. This work was supported by the New Energy and Industrial Technology Development Organization (NEDO) with a project entitled Development of Evaluation Technology for Early Introduction of Regenerative Medicine, and also by Grants-in-aid for Scientific Research from the Japan Society for the Promotion of Science, from the Ministry of Education, Culture, Sports, Science, and Technology, and from the Ministry of Health, Labor, and Welfare.

Figure legends

Figure 1. Hypoxia extended the life span of MSCs in vitro. (A) Growth profiles of MSCs under normoxic (blue triangle) and hypoxic (red triangle) conditions. (B) Expression of SA-β-gal. hBM77 cells cultured for about 100 days under normoxic (PD25) or hypoxic (PD28) conditions were stained. (C) Quantitative analyses of SA-β-gal-positive cells among four hBM cell preparations at the indicated PD. White and gray box indicate normoxic and hypoxic conditions, respectively.

Figure 2. Hypoxia down-regulated the expression of p16 in MSCs. Expression of p16 was evaluated by Western blotting using antibody for p16 protein. The relative expression level was determined using the value at PD3 of normoxic cultured-cells as a standard. White and gray box indicate normoxic and hypoxic conditions, respectively.

Figure 3. Hypoxia enhanced differentiation properties of MSCs. Each preparations of MSCs was cultured for approximately 100 days under either normoxic or hypoxic conditions and then induced to undergo (A) osteogenic, (B) chondrogenic, or (C) adipogenic differentiation under normoxic conditions. The results were quantified based on the content of Ca, GAG, or TG, respectively. PD numbers of the MSCs used for these experiments are indicated. White and gray box indicate normoxic and hypoxic conditions, respectively.

Figure 4. Hypoxia down-regulated the activation of ERK in MSCs. (A) Expression of molecules related to MAPK signaling pathways of huBM72 at the indicated PD. (B) Expression of pERK1/2 during the life span of MSCs in vitro. The relative level of pERK2 was determined using the value at PD3 of normoxic cells as a standard. White and gray box indicate normoxic and hypoxic conditions, respectively. (C) Effect of nPG treatment on the expression of HIF-1α and pERK1/2. huBM72 cells cultured under normoxic conditions at PD3 were treated with nPG at the indicated concentration for 4 h, and proteins were extracted for Western blotting. (D) Effect of a MEK inhibitor on the expression of pERK1/2 and p16. huBM72 cells cultured under normoxic conditions at PD3 were treated with U0126 (10μM) for up to 96 h, and proteins were extracted for Western blotting. The relative expression level of p16 was determined using the value of normoxic cultured-cells at 24h as a standard. White and gray box indicate normoxic and hypoxic conditions, respectively.

References

[1] A.I. Caplan, and S.P. Bruder, Mesenchymal stem cells: building blocks for molecular medicine in the 21st century. Trends Mol Med 7 (2001) 259-64.

[2] L. Mazzini, K. Mareschi, I. Ferrero, E. Vassallo, G. Oliveri, R. Boccaletti, L. Testa, S. Livigni, and F. Fagioli, Autologous mesenchymal stem cells: clinical applications in amyotrophic lateral sclerosis. Neurol Res 28 (2006) 523-6.

[3] H. Ohgushi, N. Kotobuki, H. Funaoka, H. Machida, M. Hirose, Y. Tanaka, and Y. Takakura, Tissue engineered ceramic artificial joint-ex vivo osteogenic differentiation of patient mesenchymal cells on total ankle joints for treatment of osteoarthritis. Biomaterials 26 (2005) 4654-61.

[4] W. Wagner, P. Horn, M. Castoldi, A. Diehlmann, S. Bork, R. Saffrich, V. Benes, J. Blake, S. Pfister, V. Eckstein, and A.D. Ho, Replicative senescence of mesenchymal stem cells: a continuous and organized process. PLoS One 3 (2008) e2213.

[5] K. Itahana, J. Campisi, and G.P. Dimri, Mechanisms of cellular senescence in human and mouse cells. Biogerontology 5 (2004) 1-10.

[6] S. Loft, P. Hogh Danielsen, L. Mikkelsen, L. Risom, L. Forchhammer, and P. Moller, Biomarkers of oxidative damage to DNA and repair. Biochem Soc Trans 36 (2008) 1071-6.

[7] P.A. Zuk, M. Zhu, H. Mizuno, J. Huang, J.W. Futrell, A.J. Katz, P. Benhaim, H.P. Lorenz, and M.H. Hedrick, Multilineage cells from human adipose

tissue: implications for cell-based therapies. Tissue Eng 7 (2001) 211-28.

[8] C. De Bari, F. Dell'Accio, P. Tylzanowski, and F.P. Luyten, Multipotent mesenchymal stem cells from adult human synovial membrane. Arthritis Rheum 44 (2001) 1928-42.

[9] G. Kogler, S. Sensken, J.A. Airey, T. Trapp, M. Muschen, N. Feldhahn, S. Liedtke, R.V. Sorg, J. Fischer, C. Rosenbaum, S. Greschat, A. Knipper, J. Bender, O. Degistirici, J. Gao, A.I. Caplan, E.J. Colletti, G. Almeida-Porada, H.W. Muller, E. Zanjani, and P. Wernet, A new human somatic stem cell from placental cord blood with intrinsic pluripotent differentiation potential. J Exp Med 200 (2004) 123-35.

[10] S. Bajada, I. Mazakova, J.B. Richardson, and N. Ashammakhi, Updates on stem cells and their applications in regenerative medicine. J Tissue Eng Regen Med 2 (2008) 169-83.

[11] D.C. Chow, L.A. Wenning, W.M. Miller, and E.T. Papoutsakis, Modeling pO(2) distributions in the bone marrow hematopoietic compartment. II. Modified Kroghian models. Biophys J 81 (2001) 685-96.

[12] D.P. Lennon, J.M. Edmison, and A.I. Caplan, Cultivation of rat marrow-derived mesenchymal stem cells in reduced oxygen tension: effects on in vitro and in vivo osteochondrogenesis. J Cell Physiol 187 (2001) 345-55.

[13] H. Ren, Y. Cao, Q. Zhao, J. Li, C. Zhou, L. Liao, M. Jia, H. Cai, Z.C. Han, R. Yang, G. Chen, and R.C. Zhao, Proliferation and differentiation of bone

marrow stromal cells under hypoxic conditions. Biochem Biophys Res Commun 347 (2006) 12-21.

[14] W.L. Grayson, F. Zhao, R. Izadpanah, B. Bunnell, and T. Ma, Effects of hypoxia on human mesenchymal stem cell expansion and plasticity in 3D constructs. J Cell Physiol 207 (2006) 331-9.

[15] W.L. Grayson, F. Zhao, B. Bunnell, and T. Ma, Hypoxia enhances proliferation and tissue formation of human mesenchymal stem cells. Biochem Biophys Res Commun 358 (2007) 948-53.

[16] E. Martin-Rendon, S.J. Hale, D. Ryan, D. Baban, S.P. Forde, M. Roubelakis, D. Sweeney, M. Moukayed, A.L. Harris, K. Davies, and S.M. Watt, Transcriptional profiling of human cord blood CD133+ and cultured bone marrow mesenchymal stem cells in response to hypoxia. Stem Cells 25 (2007) 1003-12.

[17] C. Fehrer, R. Brunauer, G. Laschober, H. Unterluggauer, S. Reitinger, F. Kloss, C. Gully, R. Gassner, and G. Lepperdinger, Reduced oxygen tension attenuates differentiation capacity of human mesenchymal stem cells and prolongs their lifespan. Aging Cell 6 (2007) 745-57.

[18] A.V. Molofsky, S.G. Slutsky, N.M. Joseph, S. He, R. Pardal, J. Krishnamurthy, N.E. Sharpless, and S.J. Morrison, Increasing p16INK4a expression decreases forebrain progenitors and neurogenesis during ageing. Nature 443 (2006) 448-52.

[19] V. Janzen, R. Forkert, H.E. Fleming, Y. Saito, M.T. Waring, D.M.

Dombkowski, T. Cheng, R.A. DePinho, N.E. Sharpless, and D.T. Scadden, Stem-cell ageing modified by the cyclin-dependent kinase inhibitor p16INK4a. Nature 443 (2006) 421-6.

[20] K.R. Shibata, T. Aoyama, Y. Shima, K. Fukiage, S. Otsuka, M. Furu, Y. Kohno, K. Ito, S. Fujibayashi, M. Neo, T. Nakayama, T. Nakamura, and J. Toguchida, Expression of the p16INK4A gene is associated closely with senescence of human mesenchymal stem cells and is potentially silenced by DNA methylation during in vitro expansion. Stem Cells 25 (2007) 2371-82.

[21] De-G. Yang, L. Liu, X.-Z. Zheng, Cyclin-dependent kinase inhibitior p16INK4a and telomerase may co-modulate endothelial prognitor cells senescence. Ageing Research Reviews 7 (2008) 137-46.

[22] T. Okamoto, T. Aoyama, T. Nakayama, T. Nakamata, T. Hosaka, K. Nishijo, T. Nakamura, T. Kiyono, and J. Toguchida, Clonal heterogeneity in differentiation potential of immortalized human mesenchymal stem cells. Biochem Biophys Res Commun 295 (2002) 354-61.

[23] M.F. Pittenger, A.M. Mackay, S.C. Beck, R.K. Jaiswal, R. Douglas, J.D. Mosca, M.A. Moorman, D.W. Simonetti, S. Craig, and D.R. Marshak, Multilineage potential of adult human mesenchymal stem cells. Science 284 (1999) 143-7.

[24] F. Tsukiyama, Y. Nakai, M. Yoshida, T. Tokuhara, K. Hirota, A. Sakai, H. Hayashi, and T. Katsumata, Gallate, the component of HIF-inducing

catechins, inhibits HIF prolyl hydroxylase. Biochem Biophys Res Commun 351 (2006) 234-9.

[25] A. Takahashi, N. Ohtani, K. Yamakoshi, S. Iida, H. Tahara, K. Nakayama, K.I. Nakayama, T. Ide, H. Saya, and E. Hara, Mitogenic signalling and the p16INK4a-Rb pathway cooperate to enforce irreversible cellular senescence. Nat Cell Biol 8 (2006) 1291-7.

[26] I. Carcamo-Orive, N. Tejados, J. Delgado, A. Gaztelumendi, D. Otaegui, V. Lang, and C. Trigueros, ERK2 protein regulates the proliferation of human mesenchymal stem cells without affecting their mobilization and differentiation potential. Exp Cell Res 314 (2008) 1777-88.

[27] R.K. Jaiswal, N. Jaiswal, S.P. Bruder, G. Mbalaviele, D.R. Marshak, and M.F. Pittenger, Adult human mesenchymal stem cell differentiation to the osteogenic or adipogenic lineage is regulated by mitogen-activated protein kinase. J Biol Chem 275 (2000) 9645-52.

[28] S. Peng, G. Zhou, K.D. Luk, K.M. Cheung, Z. Li, W.M. Lam, Z. Zhou, and W.W. Lu, Strontium promotes osteogenic differentiation of mesenchymal stem cells through the Ras/MAPK signaling pathway. Cell Physiol Biochem 23 (2009) 165-74.

[29] J. Liu, Z. Zhao, J. Li, L. Zou, C. Shuler, Y. Zou, X. Huang, M. Li, and J. Wang, Hydrostatic pressures promote initial osteodifferentiation with ERK1/2 not p38 MAPK signaling involved. J Cell Biochem 107 (2009) 224-32.

[30] Y. Chang, S.W. Ueng, S. Lin-Chao, and C.C. Chao, Involvement of Gas7 along the ERK1/2 MAP kinase and SOX9 pathway in chondrogenesis of human marrow-derived mesenchymal stem cells. Osteoarthritis Cartilage 16 (2008) 1403-12.

[31] Q.C. Liao, Y.L. Li, Y.F. Qin, L.D. Quarles, K.K. Xu, R. Li, H.H. Zhou, and Z.S. Xiao, Inhibition of adipocyte differentiation by phytoestrogen genistein through a potential downregulation of extracellular signal-regulated kinases 1/2 activity. J Cell Biochem 104 (2008) 1853-64.

Figure
Click here to download high resolution image

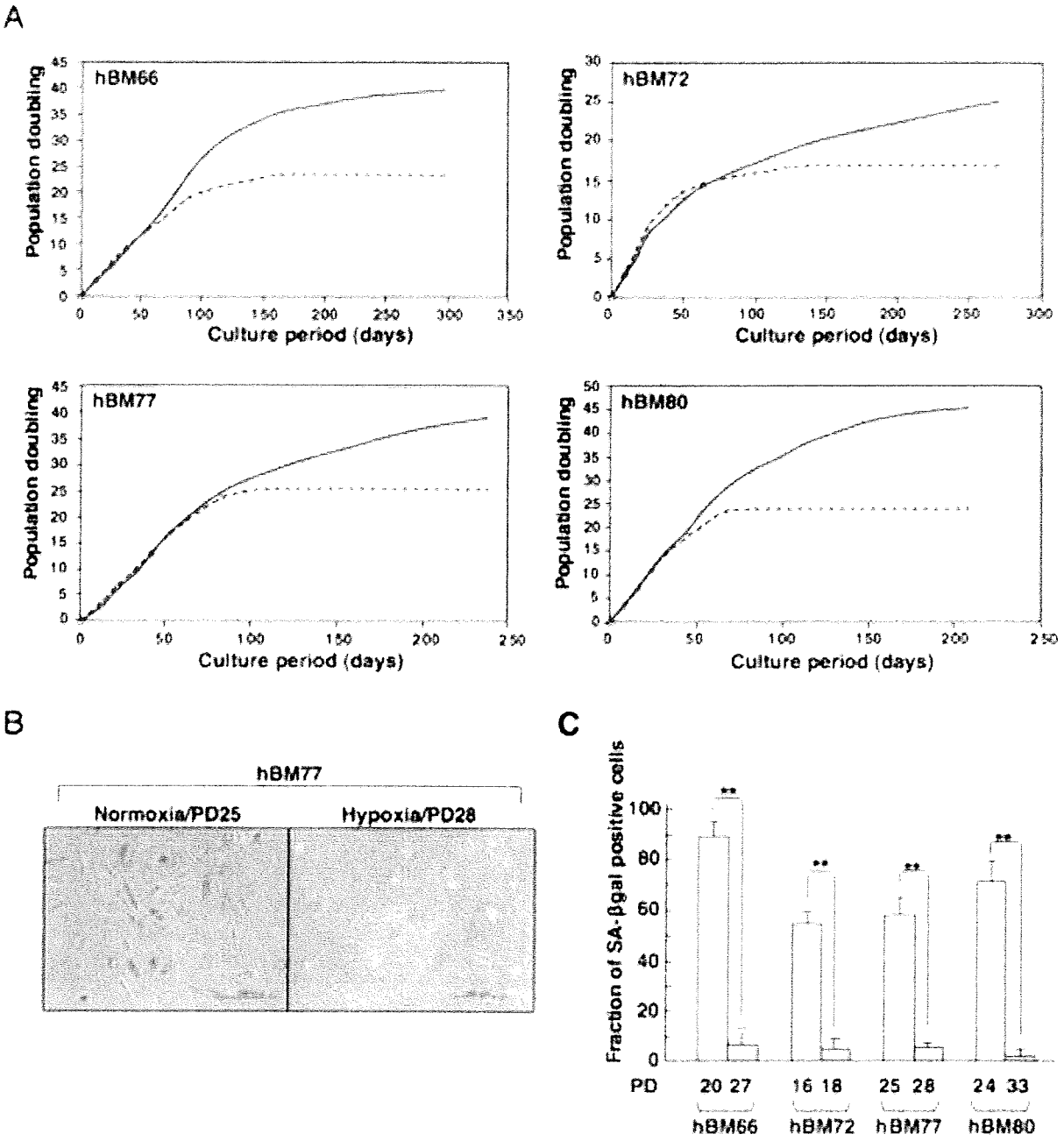

Figure
Click here to download high resolution image

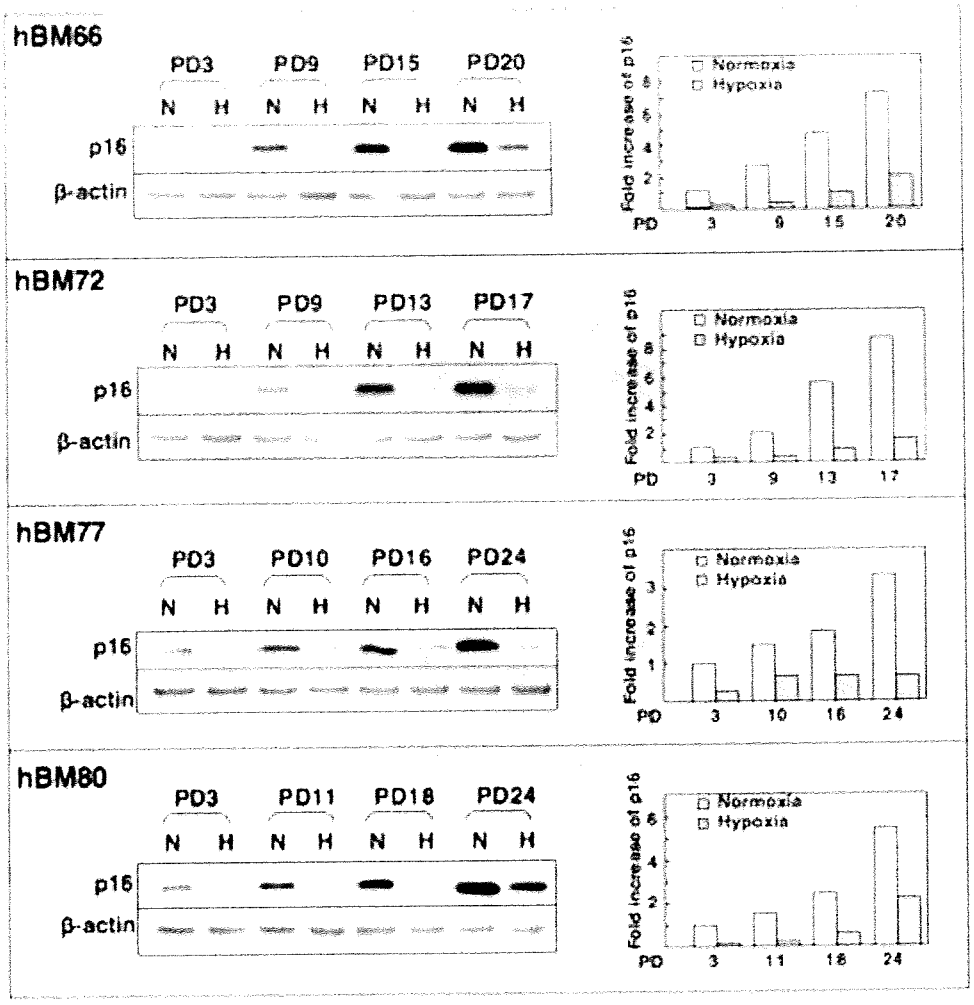

Figure
Click here to download high resolution image

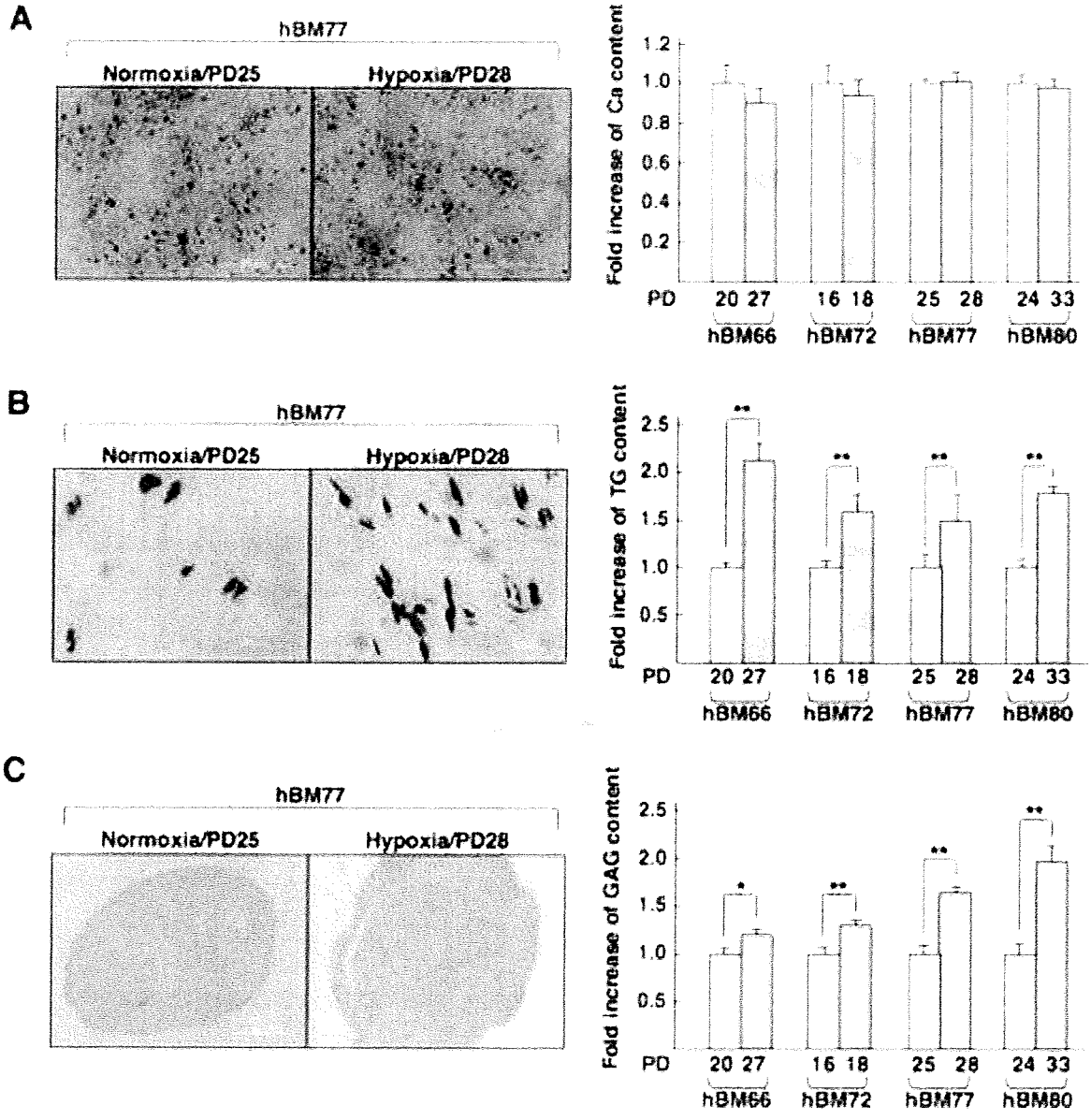

Figure
Click here to download high resolution image

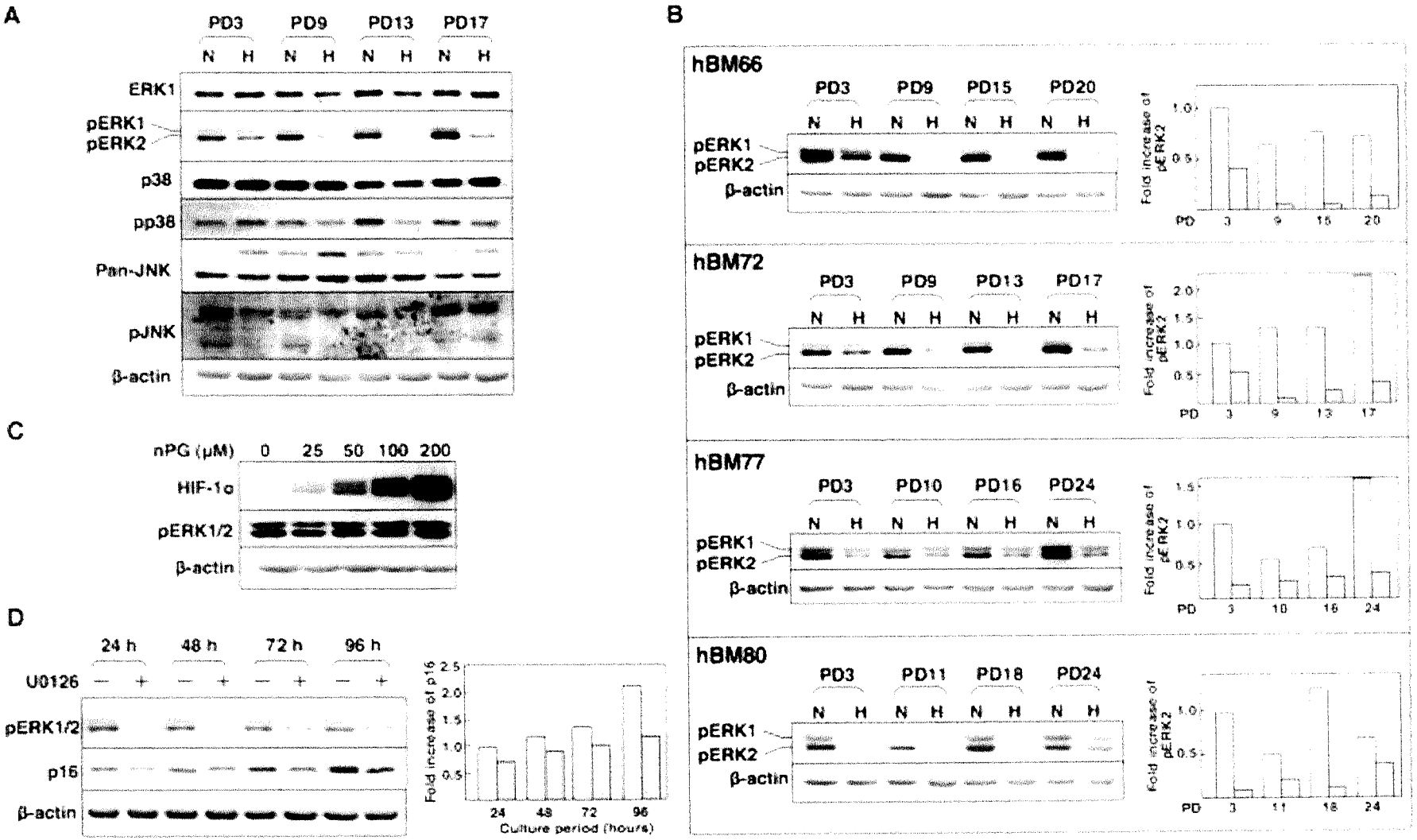

Leukemia Research 33 (2009) 649–654

Contents lists available at ScienceDirect

Leukemia Research

journal homepage: www.elsevier.com/locate/leukres

Aberrant somatic hypermutations in thyroid lymphomas

Tetsuya Takakuwa[a,*], Akira Miyauchi[c], Katsuyuki Aozasa[b]

[a] Human Health Science, Kyoto University Graduate School of Medicine, 606-8507 Sakyo-ku, Shogoin Kawahara-cyo 53, Kyoto, Japan
[b] Department of Pathology, Osaka University Graduate School of Medicine, Osaka, Japan
[c] Department of Surgery, Kuma Hospital, Kobe, Japan

ARTICLE INFO

Article history:
Received 8 May 2008
Received in revised form 6 October 2008
Accepted 7 October 2008
Available online 18 November 2008

Keywords:
Thyroid lymphoma
Follicular lymphoma
Aberrant somatic hypermutation

ABSTRACT

To determine a possible role of aberrant somatic hypermutation (ASHM) in the pathogenesis of thyroid lymphoma (TL), mutational status of genes affected by ASHM, including *c-MYC*, *PIM-1*, *PAX-5* and *RhoH/TTF*, was analyzed. Tumor specimens from 33 patients with thyroid B-cell lymphoma and 14 with chronic lymphocytic thyroiditis (CLTH), an autoimmune thyroiditis known to provide a basis for TL development, was examined. Mutations of at least one of these genes was detected in 16 of 33 (48.5%) patients with TL and in 2 of 14 (14.3%) CLTH. Occurrence of ASHM in *PIM-1*, *RhoH/TTF*, and c-*MYC* was a constant finding in follicular lymphoma (FL) (all of 11 cases) but not so frequent in diffuse large B-cell lymphoma (DLBCL) (4 (33.3%) of 12 cases) and Marginal zone B-cell lymphoma (MZBCL) (1 (10.0%) of 10 cases). ASHM activity is ongoing in most of FL and DLBCL because intraclonal variants were found. FL was also unique in its lower expression level of activation-induced cytidine deaminase, a main player in DNA-modifying processes during SHM, compare to DLBCL and MZBCL.

1. Introduction

Somatic hypermutation (SHM) in the germinal center (GC) B-cells is a process that enhances affinity of antibody for a particular antigen by introducing nucleotide substitutions within the immunoglobulin variable region (IgHV) genes [1]. SHM is characterized by the predominance of single base substitutions, preference for transitions over transversions, and specific targeting of AG/G/CT/AT (RGYW) motifs. *BCL-6* proto-oncogene, a transcriptional repressor that regulates B-cell maturation [2], is another target of SHM in GC B-cells. BCL-6 is a proto-oncogene initially cloned from 3q27 breakpoints in diffuse large B-cell lymphoma (DLBCL) of the immunocompetent host, and found to encode a zinc-finger transcriptional repressor.

An aberrant activity of SHM, called aberrant SHM (ASHM), has been suggested to contribute to the development of DLBCLs [3]. Majority of DLBCLs exhibit ASHM in the coding sequence or 5′ untranslated region (UTR) of proto-oncogenes, including *PIM-1*, *PAX-5*, *RhoH/TTF*, and c-*MYC* [3], which is implicated in the pathogenesis of lymphoid malignancies. The ASHM of these genes was reported to be commonly found in DLBCL but uncommon in other kinds of GC-derived lymphomas such as follicular lymphoma (FL) and Burkitt lymphoma. This observation might lead to the concept that ASHM plays a role for lymphomagenesis of aggressive B-cell lymphomas through mutation of multiple proto-oncogenes. Recent study, however, demonstrated that ASHM was also observed in various kinds of lymphomas, i.e., lymphoma associated with AIDS [4], primary central nervous system lymphomas [5], mediastinal DLBCL [6,7], and hepatitis C virus positive non-Hodgkin's B-cell lymphoma (B-NHL) [8], cutaneous B-cell lymphoma [9], lymphoma of marginal zone B-cell type (MZBCL) and extranodal DLBCL [10], and FL [11], suggesting that ASHM may contribute to oncogenesis in a wide spectrum of B-cell lymphomas.

Thyroid lymphoma (TL) is a minor constituent of B-NHL, accounting for 2.2–2.5% of all cases of extranodal lymphomas [12,13]. TL had attracted the attention of investigators because of its putative origin from active lymphoid cells in an organ-specific autoimmune thyroiditis, i.e., Hashimoto's thyroiditis or chronic lymphocytic thyroiditis (CLTH) [14,15]. TL exclusively comprise B-NHL with DLBCL, MZBCL and FL being frequent in the order [16]. Previous study revealed the relatively high level of SHM (1–21%, average 12%) in IgHV genes [17], and deviated VH4 Ig gene usage among MZBCL in TL [18]. In this study, biopsy specimens from 33 patients with B-NHL of thyroid and 14 CLTH patients were analyzed to evaluate occurrence of ASHM. Activation-induced cytidine deaminase (*AID*) and *POL-eta* gene, known to play central roles in the DNA-modifying processes during SHM, contribute differently and complementarily to this process [19–22] Then, expression levels of *AID* and *POL-eta* gene and their relation with the ASHM were also analyzed.

* Corresponding author. Tel.: +81 75 751 3956; fax: +81 75 751 3956.
E-mail address: tez@hs.med.kyoto-u.ac.jp (T. Takakuwa).

0145-2126/$ – see front matter © 2008 Elsevier Ltd. All rights reserved.
doi:10.1016/j.leukres.2008.10.007

2. Patients and methods

2.1. Patients

Thirty-three patients with TL and 14 with CLTH, who underwent surgical resection including total, partial thyroidectomy, or open biopsy of thyroid lesions in the Kuma Hospital, Kobe, Japan, during the period 1995–1999, were enrolled in this study with informed consent. TL patients consisted of 7 males and 26 females while CLTH patients consisted of 1 male and 13 females. Age of patients on admission ranged from 27 to 84 (median 65) years in TL and 45 to 75 (median 62.5) years in CLTH. All 33 tissue specimens were subdivided into two: one for snap-frozen at −150 °C and another for formalin fixed paraffin embedded for further analysis. Criteria for the diagnosis of CLTH included increased consistency of the thyroid-gland, occasional hypothyroidism, high level of thyroid-stimulating hormone, low ^{123}I-uptake, and the presence of antimicrosomal and/or anti-thyroglobulin antibodies in the serum. Histologic findings of CLTH included lymphocytic infiltration, usually forming lymphoid follicles with GCs, varying degrees of fibrosis and oxyphilic change or squamous metaplasia in epithelial cells of the thyroid follicles. All of the histologic sections from TL cases were reviewed by one of the authors (KA) and were classified according to the 2001 World Health Organization (WHO) Classification of Tumours of Haematopoietic and Lymphoid Tissues [16]. They included 12 DLBCLs, 10 MZBCLs, and 11 FLs. Immunohistochemical study on the paraffin sections from TL was carried out using the avidin–biotin–peroxidase complex (ABC) method. Monoclonal antibodies used for immunophenotyping were CD20, CD3, BCL-6, MUM1 (Dakocytomation, Glostrup, Denmark, dilution at 1:400, 1:50, 1:50, 1:50, respectively), and CD10 (NICHIREI BIOSCIENCES, Tokyo, Japan, used as a prediluted antibody). All TL were of B-cell lineage. Morphological and immunophenotypic analyses revealed that the fraction of malignant cells in the pathological specimen was 90% or more in all cases. DLBCL was stratified into 3 germinal center B-cell-like (GCB) and 9 non-GCB phenotypes according to the immunophenotype of CD10, BCL-6 and MUM-1 [23]. t(14;18) with BCL-2-IgH rearrangement was detected in 4 (36.4%) of 11 FL cases using the method described elsewhere [24]. Translocation t(14;18) as a hallmark of FL was reported to occur at a lower frequency, 48–55%, in Asian patients, than in the European and Northern American patients (70–95%) [16,19–25]. The reactive and non-neoplastic nature of CLTH lesions was confirmed by clonality assays [24,26].

2.2. Detection of ASHM

DNA was extracted from fresh frozen thyroid tissues, using the phenol-chloroform extraction method. Sequences of the oligonucleotide primers used for amplification of *PIM-1*, *PAX-5*, *RhoH/TTF*, exons 1 and 2 of c-*MYC*, and *BCL-6* by the polymerase chain reaction (PCR) were described elsewhere [5,8].

2.3. Analysis of PIM-1, PAX-5, RhoH/TTF, c-MYC, and BCL-6 mutations

Mutational analysis of *PIM-1*, *PAX-5*, *RhoH/TTF*, c-*MYC*, and *BCL-6* was confined to the regions where more than 90% of mutations introduced by ASHM were reported to be found in B-cell lymphomas [3,4,11]. Purified PCR products were sequenced using an ABI 3100 Genetic Analyser (Applied Biosystems, Foster City, CA, USA) with the dye-terminator protocol. Both strands of each PCR product were sequenced. The sizes of PCR products for the *PIM-1*, *PAX-5*, *RhoH/TTF*, c-*MYC* exon 1, c-*MYC* exon 2, and *BCL-6* were 1025, 932, 875, 1302, 1167, and 739 bp, respectively. The sequences of each PCR product were compared with the corresponding wild-type sequence. GenBank accession numbers of wild-type *PIM-1*, *PAX-5*, *RhoH/TTF*, c-*MYC*, and *BCL-6* sequences are AF386792, AF386791, AF386789, X00364, and AF191831, respectively.

To analyze the presence of intraclonal heterogeneity, sequencing of cloned PCR products of *PIM-1*, *PAX-5*, *RhoH/TTF* and *BCL-6* was performed using the proof-reading Pfu polymerase (Invitrogen, Rockville, MD). From each patient, 20 clones were sequenced from both sides. The mutations detected at least in two individual sequencing of each patient were considered to be ongoing mutation.

2.4. Real-time PCR for assessment of expression levels of AID and POL-eta genes

Tissue samples from TL and CLTH were homogenized, and total RNA was extracted in the presence of TRIzol reagent (Invitrogen, Rockville, MD). Five microgram of total RNA were reverse-transcribed by random hexamer priming. Expression levels of *AID* and *POL-eta* were analyzed using the TaqMan Gene Expression Assays TM according to the protocol of the manufacturer (Applied Biosystems). The primers used were: *AID*, ID Hs00221068_m1, POL-eta; Hs00197814_m1, human GAPD; 4352934E (Applied Biosystems). Standard curves for quantification of the molecules were constructed from the results of simultaneous amplifications of serial dilutions of cDNA from tonsilar tissues of healthy volunteer. Real-time PCR and subsequent calculations were carried out with an ABI Prism 7700 Sequence Detector System (Applied Biosystems). To normalize the differences in RNA degradation and RNA loading for reverse transcription-PCR in individual samples, the expression levels of each molecule were divided by that of human GAPD in the same samples. All experiments were performed at least in duplicate. The expression level of each gene in tonsil was defined as 100, and the relative gene expression levels in each case was compared.

2.5. Statistical analysis

Differences in the frequency of mutations were defined as statistically significant when the p values were less than 0.05. Mutation frequency was normalized based on the base composition of the sequences of each gene analyzed. The normalized mutation frequencies of each individual nucleotide were compared with the expected mutation frequency by Chi-square test [4]. The mutation frequency for nucleotides occurring in the context of an RGYW/WRCY motif was compared with the expected mutation frequency by the Chi-square test [4]. AID expression among histological subtypes of TL were compared by Kruskal–Wallis test then by Sheffe's F-test. Levels of AID expressions between ASHM positive and negative cases were compared by t-test.

3. Results

3.1. Frequency of ASHM in TL and CLTH

DNA extracted from the biopsy specimens from 33 TL patients and 14 CLTH patients were analyzed for mutations of *PIM-1*, *PAX-5*, *RhoH/TTF*, and *c-MYC* (Table 1). Mutations of *PIM-1*, *PAX-5*, *RhoH/TTF*, and *c-MYC* were detected in 7 (21.2%), 2 (6.1%), 7 (21.2%), and 11 (33.3%) of 33 TL patients, respectively. Mutations of at least one of these genes was detected in 16 of 33 (48.5%) TL patients and in 2 of 14 (14.3%) CLTH.

Frequency of mutations in more than one of these genes in FL (11 of 11 (100%)) was significantly higher than that in MZBCL (1 of 10 (10.0%)), DLBCL (4 of 12 (33.3%)), and CLTH (2 of 14 (14.3%)). Frequency of mutations was not different between GC (1 of 3 (33.3%)) and non-GC (3 of 9 (33.3%)) subtypes in DLBCL. Frequency of mutations in *c-MYC* and *PIM-1* was significantly higher in FL (*c-MYC*, 63.6%; *PIM-1*, 45.5%) than in MZBCL (*c-MYC*, 10.0%; *PIM-1*, 0%) and CLTH (*c-MYC*, 7.1%; *PIM-1*, 0%). Mutations of *RhoH/TTF* were significantly higher in FL (63.6%) than in MZBCL (0%), CLTH (7.1%) as well as DLBCL (0%).

3.2. Distribution of mutations in PIM-1, PAX-5, RhoH/TTF, and c-MYC in TL tissue

Characteristics of *PIM-1*, *PAX-5*, *RhoH/TTF*, and *c-MYC* mutations in each case of TL and CLTH were shown in Table 2, and their general features are summarized in Table 3. Average frequency of mutations per 1000 bp in cases with mutations ranged from 0.86 (c-MYC exon 2) to 4.35 (c-MYC exon 1). Majority of the mutations were single base-pair substitutions ($n = 58$). Deletions/insertions of a short DNA stretch were observed in three cases (Tables 2 and 3). Of the 58 single base-pair substitutions, 30 were transitions and 28 were transversions, with a transition-to-transversion ratio of 2.18 (expected 1.07, $p < 0.05$, Chi-square test; Table 3). Analysis of the nucleotide mutational pattern in *PIM-1*, *PAX-5*, *RhoH/TTF*, and *c-MYC* revealed that G + C and A + T base-pairs were equally targeted. Mutations within RGYW/WRCY motifs were more frequent than mutations without these motifs in c-MYC exon 1 ($p = 0.023$) (Table 3).

Three c-MYC mutations found in TL and one in CLTH involved the coding region. Two of these mutations would cause amino acid changes (Val → Ala in F6, Ile → Thr in H7), which result in alteration of the biochemical and structural properties of the proteins. Whereas the remaining two mutations were silent, one PIM-1 mutation in FL was located within the coding region, which would cause an amino acid change (Ala → Thr in F6), probably altering the biochemical and structural properties of the protein.

3.3. BCL-6 mutations in TL

The mutational analysis of the BCL-6 gene was also performed in all 33 TL patients. SHM of BCL-6 were detected in 22 of 33 (66.6%) cases: including 8 of 11 (72.7%) in FL, 9 of 12 in DLBCL (75.0%), 5